CONF-950150--10

LA-UR-95-2436

Title: COMPARISON AND ANALYSIS OF 2-D SIMULATION RESULTS WITH TWO IMPLOSION RADIATION EXPERIMENTS ON THE LOS ALAMOS PEGASUS I AND PEGASUS II CAPACITOR BANKS

Author(s):

Darrell L. Peterson, XPA
Richard L. Bowers, XPA
Charles F. Lebeda
Walter Matuska, XPA
John F. Benage, P-22
George Idzorek, P-22
Henn Oona, DX-15
John L. Stokes, P-22

Submitted to:

IEEE PULSED POWER
July 10-13, 1995
Albuquerque, NM

DISTRIBUTION OF THIS DOCUMENT IS UNLIMITED

MASTER

AUG 29 1995
OSTI

Los Alamos
NATIONAL LABORATORY

COMPARISON AND ANALYSIS OF 2-D SIMULATION RESULTS WITH TWO IMPLOSION RADIATION EXPERIMENTS ON THE LOS ALAMOS PEGASUS I AND PEGASUS II CAPACITOR BANKS

D. L. Peterson, R. L. Bowers, C. F. Lebeda, W. Matuska,
J. Benage, G. Idzorek, H. Oona, J. Stokes,
Los Alamos National Laboratory, Los Alamos, NM, 87545,

and N. F. Roderick,
Department of Chemical and Nuclear Engineering,
University of New Mexico, Albuquerque, NM, 87131.

Abstract

Two experiments, PegI-41, conducted on the Los Alamos Pegasus I capacitor bank, and PegII-25, on the Pegasus II bank, consisted of the implosions of 13 mg (nominal), 5 cm radius, 2 cm high thin cylindrical aluminum foils resulting in soft x-ray radiation pulses from the plasma thermalizion on axis. The implosions were conducted in direct-drive (no intermediate switching) mode with peak currents of about 4 MA and 5 MA respectively, and implosion times of about 2.5 μs and 2.0 μs. A radiation yield of about 250 kJ was measured for PegII-25. The purpose of these experiments was to examine the physics of the implosion and relate this physics to the production of the radiation pulse and to provide detailed experimental data which could be compared with 2-D radiation-magnetohydrodynamic (RMHD) simulations. Included in the experimental diagnostic suites were faraday rotation and dB/dt current measurements, a visible framing camera, an x-ray stripline camera, time-dependent spectroscopy, bolometers and XRD's. A comparison of the results from these experiments shows agreement with 2-D simulation results in the instability development, current, and radiation pulse data, including the pulsewidth, shape, peak power and total radiation yield as measured by bolometry. Instabilities dominate the behavior of the implosion and largely determine the properties of the resulting radiation pulse. The 2-D simulations can be seen to be an important tool in understanding the implosion physics.

Introduction

The magnetic implosion of cylindrical, conducting loads has been used in pulsed power experiments for decades as a source of soft x-rays.[1] The Los Alamos foil implosion effort has as a goal the development of imploding plasmas as an x-ray source with a total yield of 1 to 10 MJ in radiation energy, delivered in a pulse of greater than 100 TW power. The prime power source could be a large capacitor bank or an explosive flux-compression generator.[2] Experiments have been designed and fielded with thin (several thousand angstrom thick) cylindrical aluminum foil loads.[3, 4, 5, 6] In this paper we discuss computational modeling and the results of experiments in which aluminum loads were imploded on the Pegasus I and Pegasus II capacitor bank facilities.[7, 8]

One-dimensional models of these implosions generally predict efficient conversion of kinetic energy into x-ray output and radiation pulsewidths that are very short (typically with a full width at half maximum of about 10 ns or less for a 2 μs implosion). The imploding plasma is, however, subject to the development of magnetically driven Rayleigh-Taylor instabilities. As a result of this instability growth, the radiation pulse is broadened and the maximum power is reduced. Understanding the development of the instabilities and how they affect the radiation pulse, as well as being able to properly simulate experiments which show the effects of the instabilities, is the first step in designing implosion loads which will produce higher quality radiation pulses.

We have studied the physics of the imploding plasmas using a 2-D RMHD Eulerian code which is well suited to examining instability growth. The code uses SESAME equation-of-state tables and is self-consistently coupled to a ladder circuit network, which simulates the capacitor bank and associated power-flow hardware. There are no arbitrary adjustments to the plasma resistivity and the physics models employed are standard, the effects seen in the radiation pulse arise out of the 2-D nature of the simulation. The 2-D

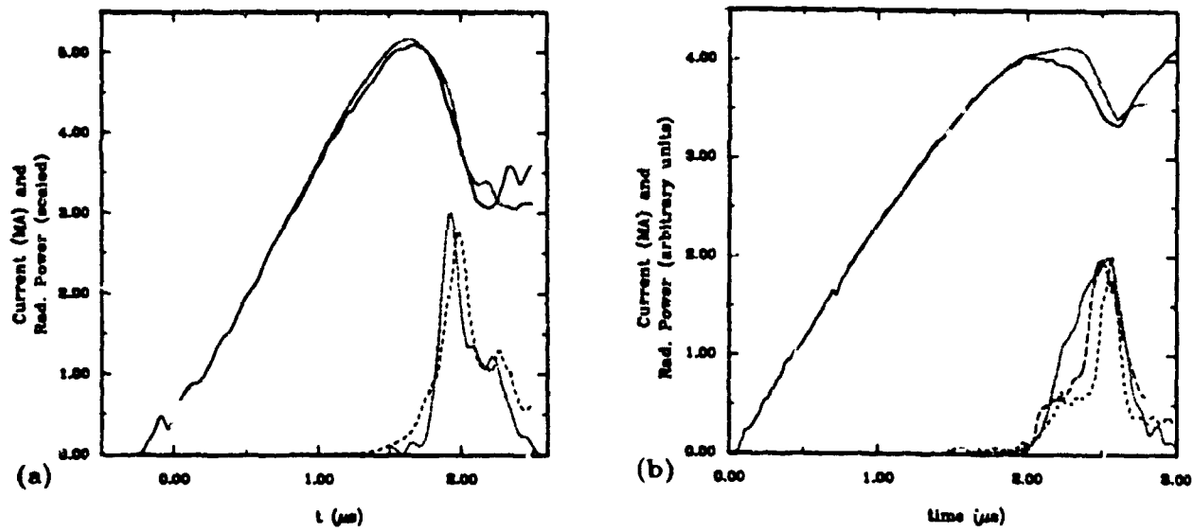

Fig. 1. (a) Experimental (solid) and 2-D simulation (dash-dot) currents and radiation powers (experimental - dotted, simulation - dashed) for the PegII-25 experiment. The experimental and calculated powers have both been scaled by a common factor to allow them to be displayed together with the currents. (b) PegI-41 experimental (solid) and 2-D simulation (dash-dot) currents with XRD data (two filterings, dotted and short dash) and the simulation radiation power (long dash). The XRD data and calculated radiation power for PegI-41 have been normalized to an arbitrary peak value of 2.0 .

simulations begin at a point after the plasma has expanded from the original thin solid foil. Perturbations in the density of the plasma are imposed to mock-up variations which arise in the experiment. These perturbations then seed the growth of magnetically driven Rayleigh-Taylor instabilities. The simulations can then be compared with experiments where the effects of the instability development are seen not only in the observed radiation pulse, but in current and voltage waveforms, in visible light framing camera photos of the imploding plasma and in time-dependent spectroscopy measurements.

PegII-25 Experiment

The PegII-25 experiment, conducted on the Pegasus II capacitor bank (an upgrade of the original Pegasus I bank) imploded a 14.32 mg pure aluminum foil. This experiment gave the largest radiation yield of any experiment in the Pegasus series, with a total of about 250 kJ as measured by bolometry. The peak current obtained was 5.1 MA. In Fig. 1a, a comparison is shown between the measured and calculated load currents, and the measured and calculated radiation powers for PegII-25. The peak powers have been scaled by a common factor to allow them to be displayed in the same figure as the currents. The peak measured radiation power is 0.83 TW and the calulated peak power is 0.76 TW. The total radiated energies are similar, with a measured value of 250 kJ and a calculated value of about 280 kJ. It can be seen that the general pulse shape and duration are similar for the measured and calculated radiation pulses.

The 2-D simulation which was used for the comparison in Fig. 1a began at $t = 0.74$ μs with a random perturbation in the density of a 3 mm thick, 2 cm long Al plasma shell. The density perturbations ranged between -15% and +15% of the average plasma density. The dynamics of the resulting magnetically driven Rayleigh-Taylor instability growth shows an evolution from short to long wavelengths and an eventual breakthrough of the plasma shell by "bubble" regions and finally a re-acceleration of "spike" material. In Fig. 2, a comparison is shown of the implosion as seen by a visible light framing camera and the corresponding development of instabilites in plasma density from the simulation. Examination of Fig. 2 reveals the classic spike-and-bubble pattern of Rayleigh-Taylor instability growth arising from the acceleration of a heavy fluid (the plasma cylinder) by a light fluid (the magnetic field). The horizontal striations which can be seen in the first two photos ($t = 1.32$ μs and 1.48 μs) are indicative of the cylindrical nature of the instability growth (the instabilities grow in the r-z plane and the density enhancements and depletions circle around the plasma

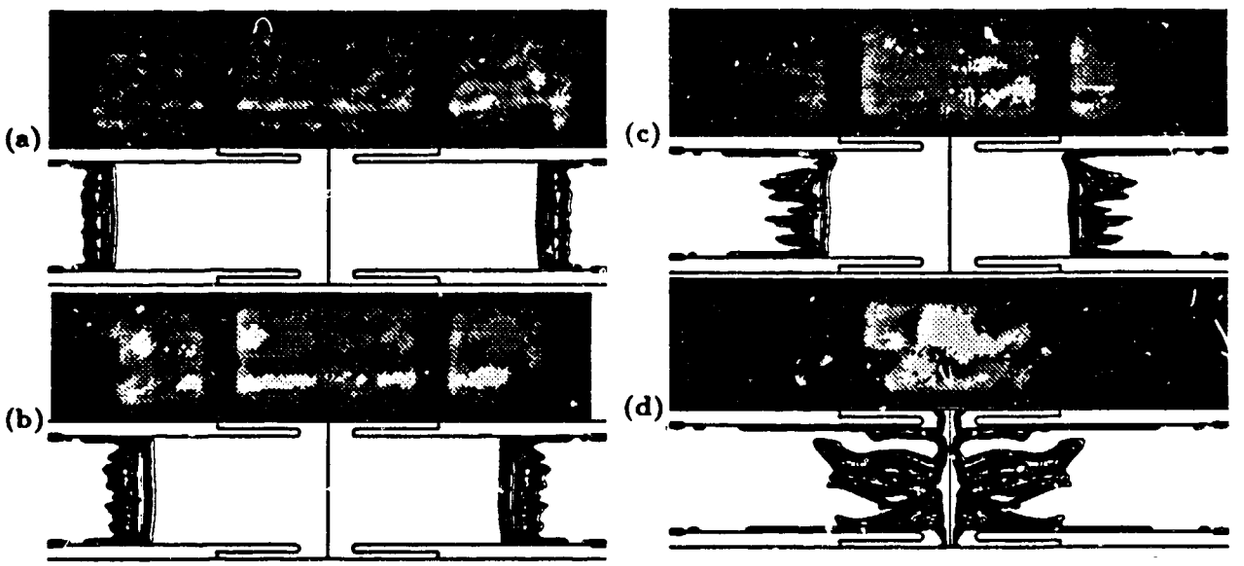

Fig. 2. Comparison of instability development as indicated by visible light framing camera photographs (above) and calculated density contours (below) at four times during the implosion: (a) $t = 1.32\ \mu s$; (b) $t = 1.48\ \mu s$; (c) $t = 1.65\ \mu s$; and (d) $t = 1.82\ \mu s$. The view is side-on with the plasma extending 2 cm in height in the vertical direction and originally 10 cm in diameter in the horizontal direction. The vertical black rectangles in the photos are return conductor vanes which obscure part of the view. A dark hemisphere seen in the lower right in the photos is a magnetic probe extending upward from the lower electrode.

in the θ direction).

Similar structure in wavelength and amplitude can be seen in the photos and density contours shown in Fig. 2. At the earliest time shown, the instabilities are short in wavelength ($\lambda \approx .33\ cm$) and have grown to only a small fraction of the plasma shell thickness (though well into nonlinear development). By the next time shown, the wavelength has increased ($\lambda \approx .5\ cm$) and the instability amplitude is an appreciable fraction of the shell thickness. In the third time shown ($t = 1.65\ \mu s$) spike material has been left behind at both electrodes with two bubble regions and a single spike near the center (most clearly seen on the left edge of the photo). Near the upper electrode, a fast growing bubble region is beginning to penetrate through the plasma shell with a spike region immediately below the bubble. In the calculation, two smaller spike regions near the lower electrode are merging and a somewhat slower developing bubble region is beginning to form which will press inward somewhat later than the top bubble. An effect from the instabilities can be seen by this time in the current waveform (Fig. 1a) which has peaked and the increased inductance from the penetrating bubbles is causing the current to decline (in unperturbed calculations the current continues to rise at this time). Finally, at $t = 1.82\ \mu s$, the bubble located near the top electrode has accelerated material to the axis and the radiation pulse has begun. Spike material in the center now extends in an "angel wing" shape (partially obscured by return conductor vanes in the photo) and a second bubble region is pressing material near the lower electrode to the axis where it will also contribute to the radiation pulse.

The combination of three dissimilar measurements, drive current, radiation bolometry and visible light photographs, which all correlate well with the results and features seen in the 2-D simulation suggest that this experiment is well modeled by the simulation. Such calculations can then be analyzed to examine the underlying physics of the production of the radiation pulse in the simulations with a view to explaining the experimental results and designing future experiments which yield radiation pulses with improved powers, durations or other tailoring of the yield. Such an analysis is illustrated in the next section.

PegI-41 Experiment

An earlier experiment, PegI-41, conducted on the Pegasus I bank imploded a 13.38 mg Al foil. A comparison of the experimental and simulation currents and radiation pulses for this experiment is shown

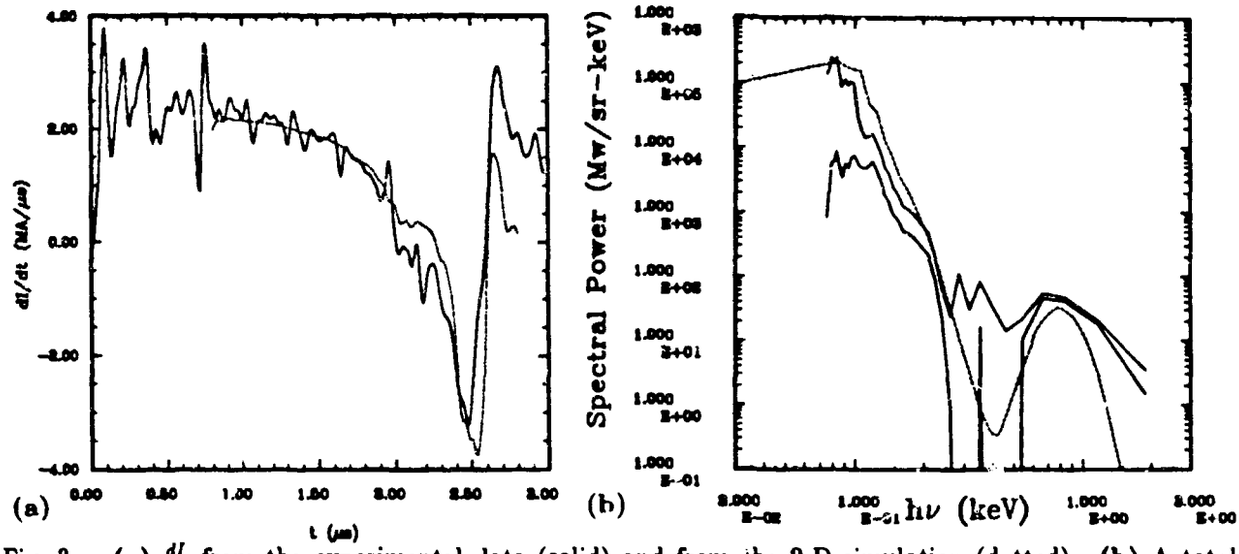

Fig. 3. (a) $\frac{dI}{dt}$ from the experimental data (solid) and from the 2-D simulation (dotted). (b) A total calculated spectrum (dotted) at $t = 2.62\ \mu s$ compared with two interpretations of the spectrometer data (solid lines).

in Fig. 1b. Bolometry and framing camera picture data are not available for this experiment, but a time-dependent spectrometer was fielded. The 2-D simulation used here began at $t = 0.8\ \mu s$ with a perturbation consisting of "notches" of depleted density on the outer radius of the expanded plasma shell, but similar results have also been obtained using random density perturbations similar to those described for the PegII-25 simulation. In Fig. 1b, the calculated radiation power is compared with data from two XRD's with different filters. The peaks of the XRD data and the radiation power have been normalized to an arbitrary value of 2.0, and thus the comparison can only be made in the pulse shape features and duration. An examination of the current data shows the presence of two inflections in the current trace during the production of the radiation pulse, corresponding to an early plateau of radiation power followed by a later peak, and similar behavior is seen in the 2-D simulation current and radiation pulse. A comparison shown in Fig. 3a of $\frac{dI}{dt}$ and in Fig. 3b of a late time ($t = 2.62\ \mu s$) spectra with the results of the 2-D simulation. Features in this spectra are correlated with material and temperatures at different locations resulting from the instability growth.[9]

An examination of the development of the instabilities in the density and rB_θ contours for this simulation shows that the instabilities have broken through the plasma shell at about $t = 2.0\ \mu s$ accelerating bubble material to the axis which in turn causes the onset of the radiation pulse. This is correlated with a marked change in $\frac{dI}{dt}$. Later, at about $t = 2.4\ \mu s$, the magnetic field contours show current flowing through spike regions that had been drifting behind the bubble regions, and it is this re-acceleration of the majority of the mass of the implosion which results in the final radiation peak and correlates to the second major change in $\frac{dI}{dt}$.

By examining the detailed information provided by the 2-D code, this process can be seen in more detail. In Fig. 4a, the operator-split nature of the code has been exploited to examine the flow of energy. In each code cycle, an edit has recorded the rate at which energy, originally deposited in the magnetic field at the beginning of the cycle, is then partially transferred into kinetic energy. The early-time behavior, before instabilities disrupt the imploding shell, is very similar to that seen in unperturbed implosions. As the bubbles burst through the shell there is a period of time when this rate no longer climbs, followed by a period of time when the re-acceleration results in a much higher rate of transfer to kinetic energy. In Fig. 4b, the total voltage across the load as registered by the code has been used to examine the effect of various processes in the implosion. The calculated voltage, which corresponds well with the inferred experimental voltage at the load and shows similar features to the radiation pulse, has been divided into three components:

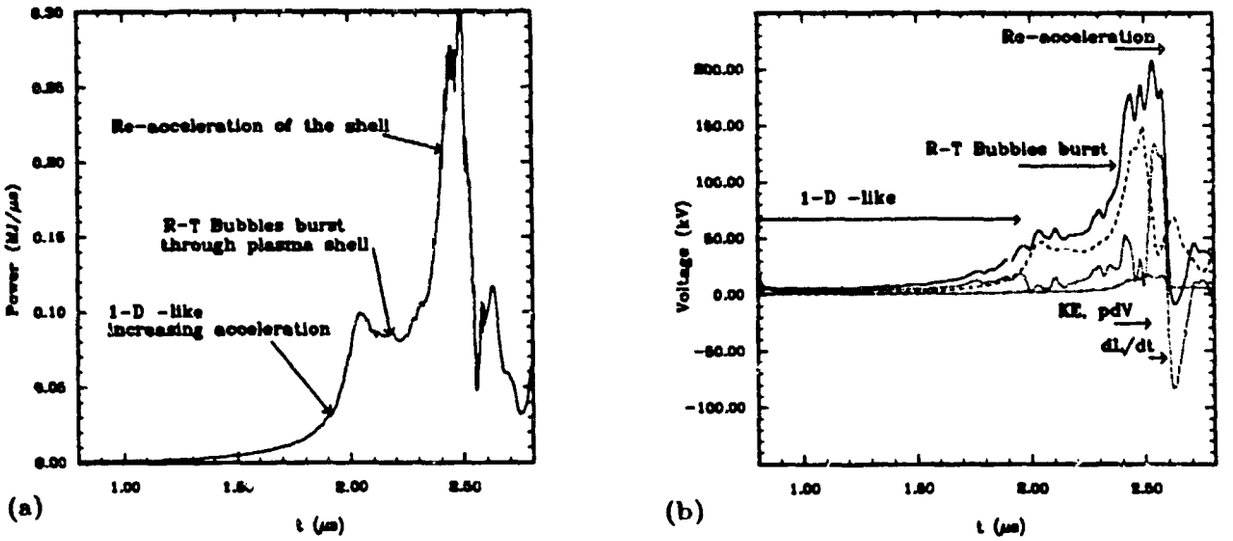

Fig. 4. (a) Rate of energy transfer from the magnetic field to kinetic energy (internal code edit for each cycle). (b) Contributions to the calculated voltage (solid) in the 2-D simulation of PegI-41. The contributions represent the effect of energy changes in the magnetic field (dotted), deposition of energy through joule heating (dot-dash), and all other energy changes (dashed).

$$
\begin{aligned}
V &= \frac{P_{Poynting}}{I} \\
&= \frac{P_{MagField}}{I} + \frac{P_{Joule}}{I} + \frac{P_{Other}}{I} \\
&= V_{MagField} + V_{Joule} + V_{Ideal} \quad .
\end{aligned}
$$

These components represent those parts of the voltage associated with changes in energy in the magnetic field ($V_{MagField}$), deposition of energy through joule heating (V_{Joule}) and all other processes such as kinetic energy change and pdV work (labeled V_{Ideal}). It can be seen immediately that resistivity plays a relatively small effect compared to the overall deposition of energy in the problem. During the 1-D -like phase of the implosion, energy is distributed relatively equally between the material and magnetic field energies. During the "plateau" region when the bubbles burst, the energy is deposited at a relatively constant rate and the fraction of the energy deposited into the magnetic field is reduced. Later, during the period of re-acceleration the voltage peak results from changes to processes such as kinetic energy increase and pdV work, followed by a brief period when the energy deposition in the magnetic field increases dramatically. Corroborating analyses have been done on this simulation examining other code quantities (such as the average mass and current radii).

Conclusions

The close agreement between disparate physical measurements and 2-D simulation results such as are seen in the simulation of PegII-25 give credence to the use of such simulations for the purpose of understanding and designing implosion experiments. By using the detail provided by such simulations it is possible to trace the effect of various physical processes which lead from instability development to the structure and duration of the calculated radiation pulse and other quantities of interest, such as the spectrum of the pulse. This will allow a deeper understanding of how changes made in parameters in the simulations (such as plasma

mass or electrode shape) can effect the resulting radiation pulse and allow for the development of designs for future experiments with a goal of improved or tailored radiation output.

References

1. F. J. Turchi and W. L. Baker, "Generation of high-energy plasmas by electromagnetic implosion," J. Appl. Phys. 44(11), 4963, Nov. 1973.

2. J Brownell, J. Parker, R. Bartsch, J. Benage, R. Bowers, J. Cochrane, P. Forman, J. Goforth, A. Greene, H. Kruse, J. Ladish, H. Oona, D. Peterson, R. Reinovsky, N. Roderick, J. Trainor and P. Turchi, "The Los Alamos Foil Implosion Project," Proceedings of the 9th International Conference on High-Power Particle Beams, Washington, D.C., May 25-29, 1992.

3. D. L. Peterson, R. L.Bowers, J. H. Brownell, A. E. Greene, H. Lee and W. Matuska, "Two-Dimensional Simulation of Foil Implosion Experiments on the Los Alamos Pegasus Capacitor Bank," AIP Conference Proceedings 299, Dense Z-Pinches, Third International Conference, London, United Kingdom 1993, 388.

4. R. L. Bowers, J. H. Brownell, A. E. Greene, H. Kruse, H. Oona and D. L. Peterson, "Nonlinear Interaction of Magnetohydrodynamic Instabilities in Radially Imploded Plasmas," Sixth International Conference on Megagauss Magnetic Field Generation and Pulsed Power Applications, Albuquerque, New Mexico, Nov. 8-11, 1992, 777

5. D. L. Peterson, R. L. Bowers, J. H. Brownell, A. E. Greene, H. W. Kruse, H. Lee and W. Matuska, "Radiation Magnetohydrodynamic Modeling of X-ray Output from Perturbed Plasma Implosions," Sixth International Conference on Megagauss Magnetic Field Generation and Pulsed Power Applications, Albuquerque, New Mexico, Nov. 8-11, 1992, 897.

6. H. Oona R. L. Bowers, D. L. Peterson, C. Findley, J. C. Cochrane and J. S. Ladish, "Experimental Studies of Instabilities in Radially Imploding Plasmas," Sixth International Conference on Megagauss Magnetic Field Generation and Pulsed Power Applications, Albuquerque, New Mexico, Nov. 8-11, 1992, 889.

7. J. C. Cochrane, R. R. Bartsch, F. Begay, H. W. Kruse, H. Oona, J. V. Parker and P. J. Turchi, "Foil Implosion Studies on Pegasus," Digest of Technical Papers, Seventh IEEE Pulsed Power Conference, Monterey, California, June 11-14, 1989, 979.

8. J. C. Cochrane, R. R. Bartsch, J. F. Benage, P. R. Forman, R. F. Gribble, M. Y. P. Hockaday, R. G. Hockaday, J. S. Ladish, H. Oona, J. V. Parker, J. S. Schlachter and F. J. Wysocki, "Direct Drive Foil Implosion Experiments on Pegasus II," AIP Conference Proceedings 299, Dense Z-Pinches, Third International Conference, London, United Kingdom 1993, 381.

9. W. Matuska, H. Lee, R. Hockaday and D. Peterson, "Source to Detector Spectrum Transformation and its Inverse for the Pegasus Z-Pinch," AIP Conference Proceedings 299, Dense Z-Pinches, Third International Conference, London, United Kingdom 1993, 525.